

# ADVANCED ELECTRONIC MATERIALS

---

Open Access

## Supporting Information

for *Adv. Electron. Mater.*, DOI 10.1002/aelm.202300693

Impact of Non-Stoichiometric Phases and Grain Boundaries on the Nanoscale Forming and Switching of HfO<sub>x</sub> Thin Films

*Niclas Schmidt, Nico Kaiser, Tobias Vogel, Eszter Piros, Silvia Karthäuser, Rainer Waser, Lambert Alff and Regina Dittmann\**

# **Supporting Information to: Impact of Non-Stoichiometric Phases and Grain Boundaries on the Nanoscale Forming and Switching of HfO<sub>x</sub> Thin Films**

Niclas Schmidt<sup>1,2</sup>, Nico Kaiser<sup>3</sup>, Tobias Vogel<sup>3</sup>, Eszter Piros<sup>3</sup>, Silvia Karthäuser<sup>1</sup>,  
Rainer Waser<sup>1,4</sup>, Lambert Alff<sup>3</sup>, and Regina Dittmann\*<sup>1</sup>

<sup>1</sup>Peter Grünberg Institute (PGI-7) and JARA-FIT, Forschungszentrum Jülich  
GmbH, 52425 Jülich, Germany

<sup>2</sup>Faculty 1 - Mathematics, Computer Science and Natural Science, RWTH Aachen  
University, 52062 Aachen, Germany

<sup>3</sup>Advanced Thin Film Technology Division, Institute of Materials Science, TU  
Darmstadt, 64287 Darmstadt, Germany

<sup>4</sup>Institute of Materials in Electrical Engineering and Information Technology (IWE  
2), RWTH Aachen University, 52056 Aachen, Germany

December 04, 2023

Email address: [r.dittmann@fz-juelich.de](mailto:r.dittmann@fz-juelich.de)

*Keywords: Hafnium oxide, resistive switching, defect engineering, grain boundaries, c-AFM, MBE*

## S1 XRD Measurements for Hf(1.2) to Hf(0.1)

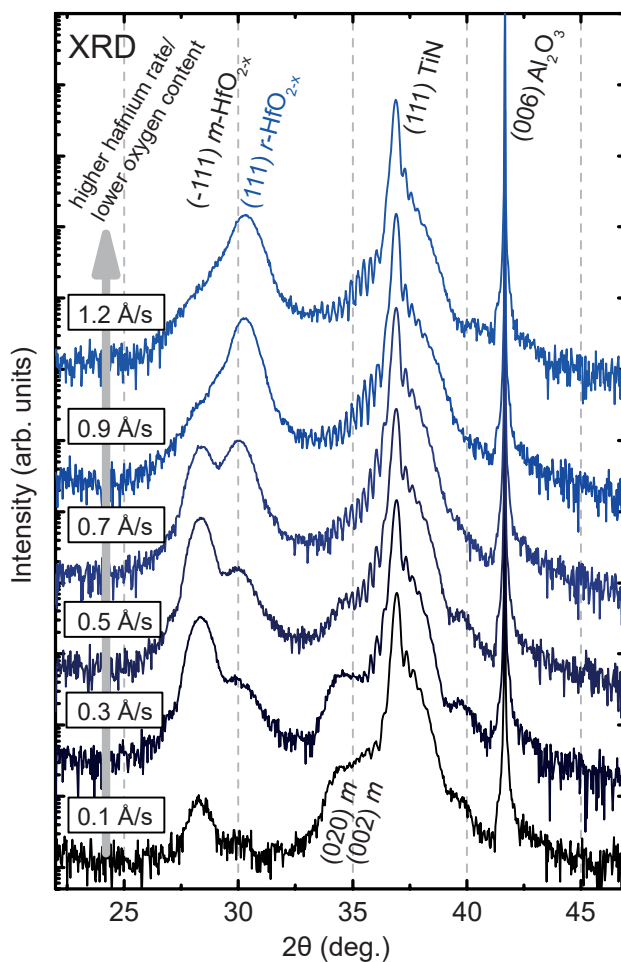


**Figure S1.**  $2\theta/\omega$  XRD measurements show the phase transition from  $m\text{-HfO}_2$  to oxygen vacancy stabilized  $r\text{-HfO}_{1.7}$  by changing the hafnium deposition rate, while maintaining constant oxygen flow and plasma energy during MBE deposition. The Laue oscillations of the TiN layer indicate high quality epitaxial film growth through highly coherent lattice planes. The (006)  $\text{Al}_2\text{O}_3$  reflection was used for alignment.

## S2 Topography TiN Substrate

An exemplary AFM topography of the 34 nm epitaxial TiN layer grown on c-cut  $\text{Al}_2\text{O}_3$  with a root mean square roughness (RMS) of  $\text{RMS} = 0.59 \text{ nm}$  is presented in Figure S2.

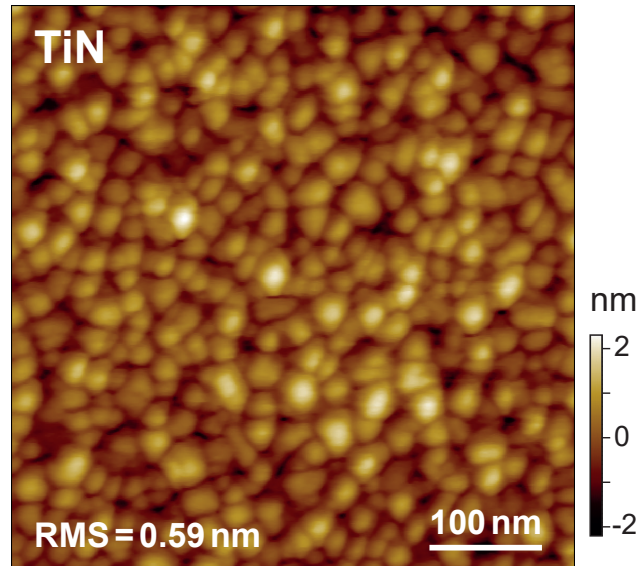


**Figure S2.** AFM topography of TiN substrate with a root mean square roughness of 0.59 nm measured over the 500 nm by 500 nm image.



### S3 Topography for Hf(1.2) to Hf(0.1)

The topography including a height profile along the dashed line for all investigated samples is shown in Figure S3. The RMS values taken over the whole scan area (500 nm by 500 nm) vary between 0.99 nm for sample Hf(1.2) and 0.61 nm for sample Hf(0.1). Furthermore, the watershed grain analysis for corresponding topographies is given with the distribution of the mean grain diameter plotted underneath, assuming circular shaped grains. The mean value  $\mu_{\text{Dia}}$  for the normal distributed grain diameter has its minimum at 25.27 nm for sample Hf(0.7) and its maximum at 27.96 nm for sample Hf(0.3). Both, the RMS values and the grain diameters exhibit no trend with the changes in growth rate of Hf and the resulting phases of the different samples determined by XRD. Thermal effects, such as drift, are not completely negligible since all measurements are performed at room temperature. The RMS values and the mean diameter of the analyzed grains are summarized in Table S1 for all samples.

**Table S1.** Root mean square roughness and mean diameter of analyzed grains for HfO<sub>2-x</sub> thin film samples according to acquired AFM data.

<b>Sample</b>	<b>Roughness nm</b>	<b>Diameter nm</b>
Hf(0.1)	0.61	25.97
Hf(0.3)	0.84	27.96
Hf(0.5)	0.77	27.75
Hf(0.7)	0.86	25.27
Hf(0.9)	0.89	26.01
Hf(1.2)	0.99	27.33
<b>Mean Best Value</b>	<b>0.83 ± 0.12</b>	<b>26.72 ± 1.01</b>

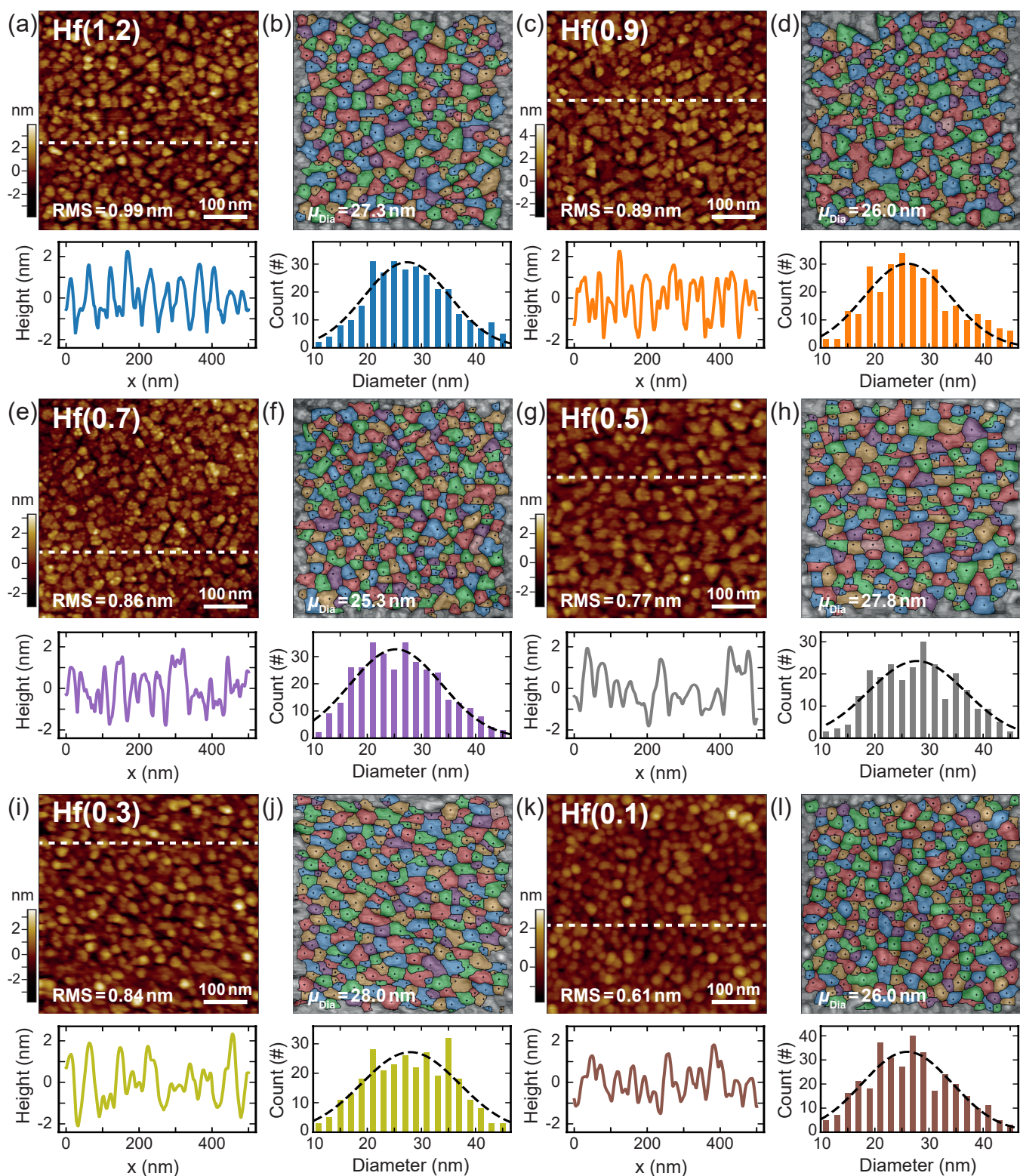


**Figure S3.** AFM topography including RMS roughness over the whole scan area with height profile along the dashed line for each  $\text{HfO}_{2-x}$  sample. Besides topography images the corresponding watershed grain analyses with mean values of the grain diameter,  $\mu_{\text{Dia}}$ , and distributions of the grain diameter are shown for samples (a,b)  $\text{Hf}(1.2)$ , (c,d)  $\text{Hf}(0.9)$ , (e,f)  $\text{Hf}(0.7)$ , (g,h)  $\text{Hf}(0.5)$ , (i,j)  $\text{Hf}(0.3)$ , and (k,l)  $\text{Hf}(0.1)$ .

## S4 Voltage Series on Hf(1.2)

The complete voltage series in addition to Figure 3 in the main manuscript for sample Hf(1.2) is shown in Figure S4. Figure S4(a) and (k), as the first and last topographies within the series, demonstrate, that the surface remains unchanged during the scans. Therefore, only the current is rising with increasing SET voltages for (b)–(j). At a voltage of  $V_{\text{set}} = 2.25 \text{ V}$  the whole scan area of Hf(1.2) turns fully conductive.

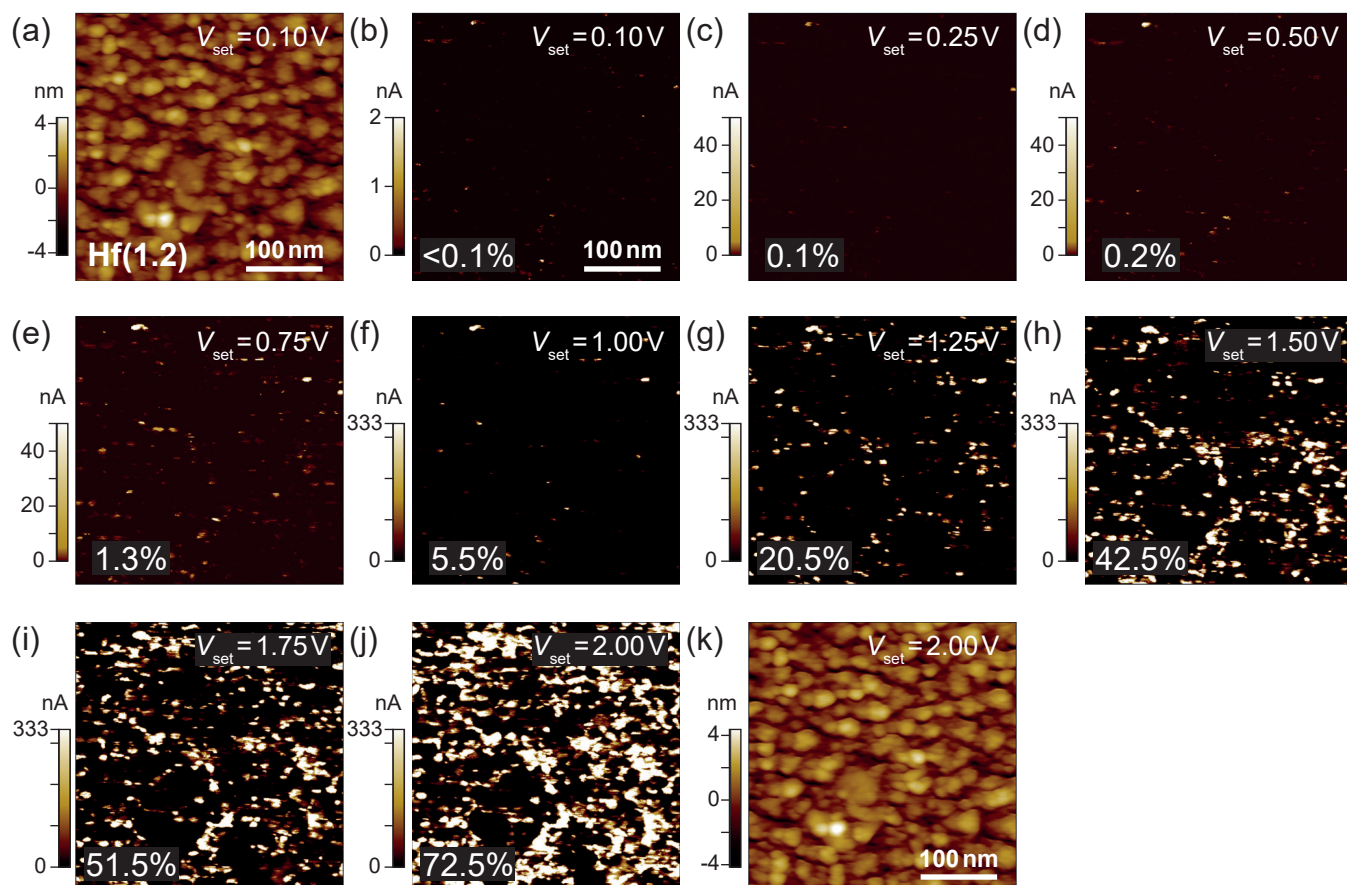


**Figure S4.** Conductive AFM topography and corresponding current maps for different SET voltages for sample Hf(1.2). (a) AFM topography for the first SET voltage  $V_{\text{set}} = 0.10 \text{ V}$ . (k) AFM topography for the last SET voltage  $V_{\text{set}} = 2.00 \text{ V}$ . The surface and the corresponding roughness for the scan area remains unchanged (RMS = 1.0 nm). (b)–(j) Current maps for SET voltages between  $V_{\text{set}} = 0.10 \text{ V}$  and  $V_{\text{set}} = 2.00 \text{ V}$ . The percentage of the area with a current above 2 nA is given in the lower left corner of the current maps.

For the comparison of the normalized conductive area in Figure 3(e) the area with a current above 2 nA is evaluated. The conductive area of the current maps is given in Figure S4(b)–(j). Subsequently, the values are normalized on the area with a current  $>2 \text{ nA}$  of the current map acquired with the highest possible voltage that can be applied to the respective sample within the measurement limits. The normalization is exemplary summarized for Hf(1.2) in Table S2. For Hf(1.2) the whole surface is conductive at the highest SET voltage. With the analogously evaluated values for samples Hf(0.9) to Hf(0.5) the dependence of the

conductive area on the applied SET voltage is depicted in Figure 3(e). The samples, which show the current onset at the lowest voltages, have the highest amount of the rhombohedral phase.

**Table S2.** Normalization of the conductive area exemplary for Hf(1.2). Voltage with corresponding conductive area with current above 2 nA. Min-max normalized conductive area with the highest SET voltage as reference.

SET Voltage V	Conductive Area %	Normalized Conductive Area
0.10	< 0.1	0.00
0.25	0.1	< 0.01
0.50	0.2	< 0.01
0.75	1.3	0.01
1.00	5.5	0.06
1.25	20.5	0.21
1.50	42.5	0.43
1.75	51.5	0.52
2.00	72.5	0.73
2.25	100	1.00

For samples Hf(1.2) and Hf(0.9) a few spots with a current above 2 nA can be detected even for the lowest SET voltage. For Hf(0.7) and Hf(0.5) no current is measured at the minimum values of the normalized conductive area in Figure 3(e).



## S5 Spatially Resolved Current Onset

The current maps superimposed onto the topography for sample Hf(1.2) for all SET voltages with resulting currents above 2 nA are presented in Figure S5.

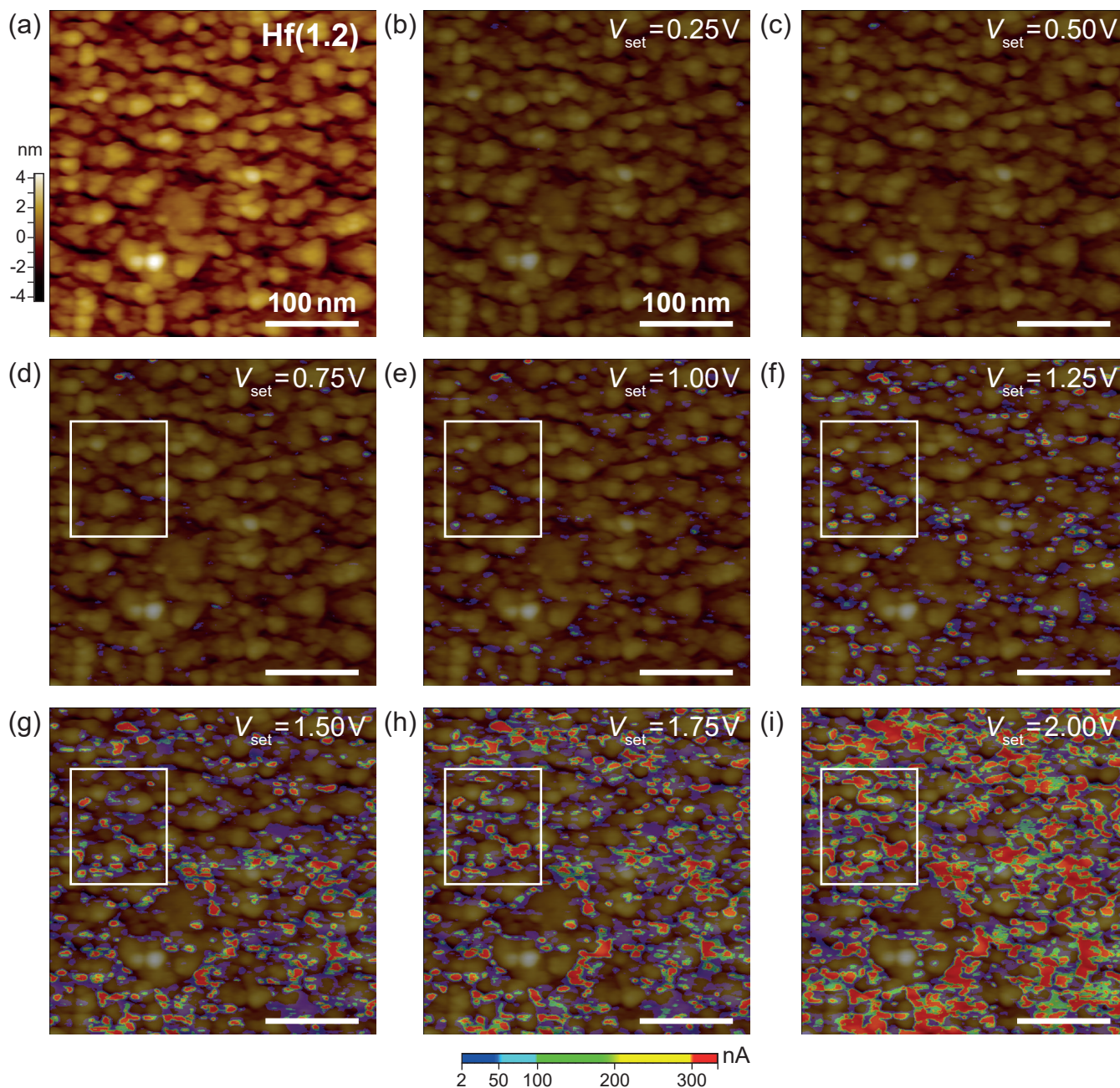


**Figure S5.** Conductive AFM topography (a) superimposed with simultaneously taken current maps for sample Hf(1.2) acquired with SET voltages of (b) 0.25 V, (c) 0.50 V, (d) 0.75 V, (e) 1.00 V, (f) 1.25 V, (g) 1.50 V, (h) 1.75 V, and (i) 2.00 V. The bottom color scale applies for current maps in images (b)–(i). Current is visualized above 2 nA. The scale of the topography in the background is the same as in (a). The white rectangles mark the excerpt in Figure 4. The scale bar in all images is 100 nm.

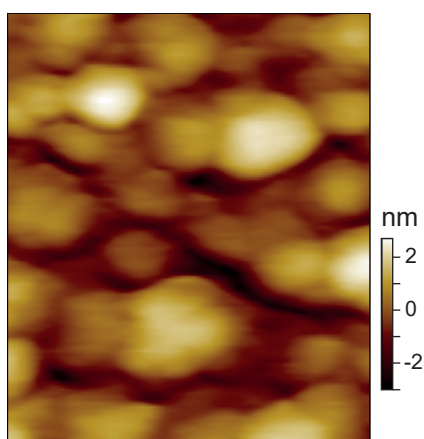


**Figure S6.** Conductive AFM topography background in Figure 4, corresponding to the marked area in Figure S5. Area: 100 nm by 120 nm.

## S6 Conductive AFM Mapping with Single Crystal Diamond Cantilever

For the comparison of the two types of used cantilevers and in order to compare the positions of first appearing current, the samples were also scanned with the single crystal diamond cantilever. Even though the cantilever has a significant smaller radius ( $<5\text{ nm}$ ) compared to the PtIr-cantilever ( $<25\text{ nm}$ ), the observations match for both probes. Current is first detected at the grain boundaries, as shown in Figure S7 exemplary for sample Hf(0.9) for a SET voltage of  $V_{\text{set}} = 1.5\text{ V}$ .

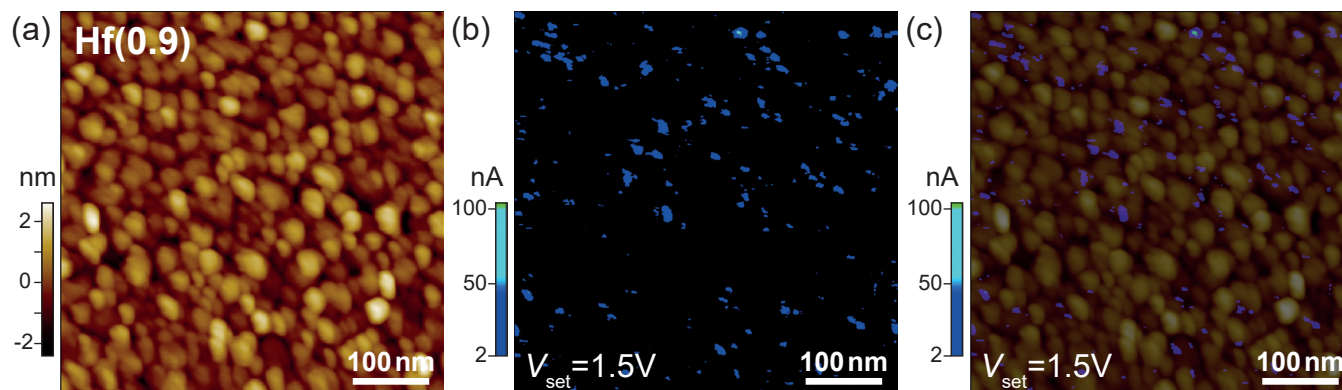


**Figure S7.** Conductive AFM measurement of sample Hf(0.9) with single crystal diamond cantilever (radius  $<5\text{ nm}$ ). (a) Topography with (b) simultaneously acquired current map with SET voltage of  $1.5\text{ V}$ , and (c) current map superimposed onto topography. Current is visualized above the threshold of  $2\text{ nA}$ .

## S7 Forming Voltage for Single Grains

In addition to Figure 5 in the main manuscript, the forming voltages for all investigated  $\text{HfO}_{2-x}$  samples are shown in Figure S8. No trend of  $V_{\text{form}}$  with the relative grain height can be observed for all samples. The mean forming voltage for each sample is marked by the dashed line.

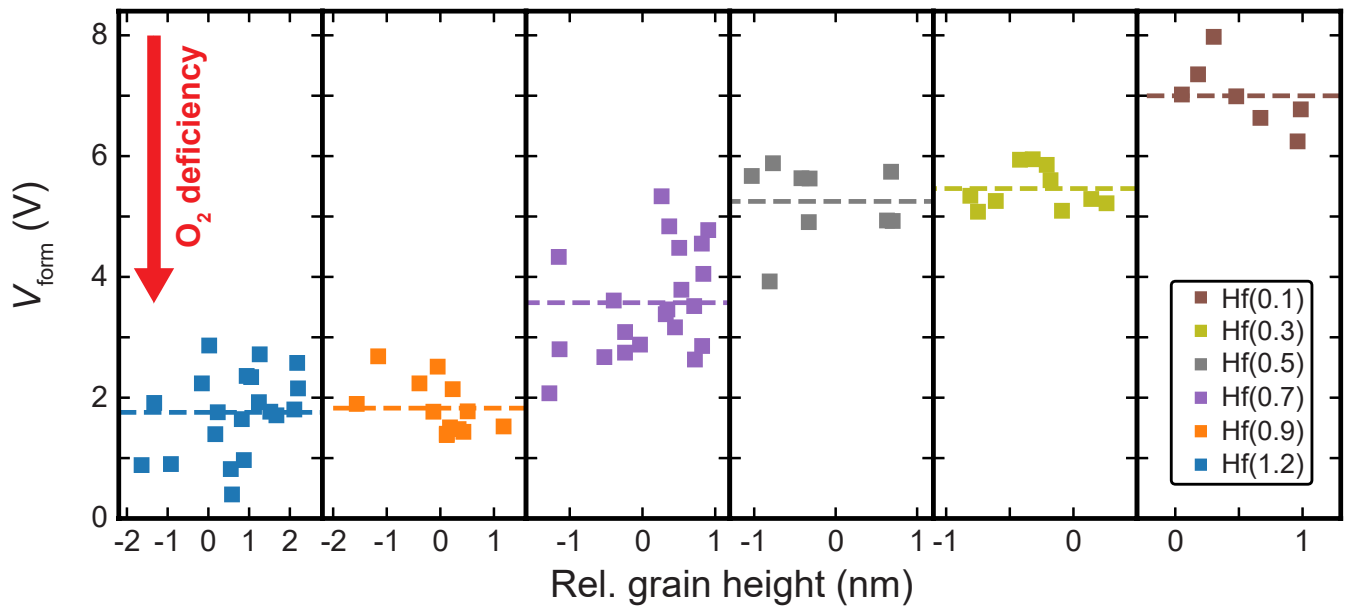


**Figure S8.** Forming voltage  $V_{\text{form}}$  of single grains for all investigated  $\text{HfO}_{2-x}$  samples with respect to the relative grain height. The mean forming voltage for each sample is marked by the dashed line.